Original Article
Yonsei Med J 2021 Jul;62(7):622-630
https://doi.org/10.3349/ymj.2021.62.7.622
Yonsei Medical Journal
YMJ
pISSN: 0513-5796 · eISSN: 1976-2437

Expression of Organic Anion Transporting Polypeptides in an H-Ras 12V Transgenic Mouse Model of Spontaneous Hepatocellular Carcinoma

Honsoul Kim[1,2*], Junjeong Choi[3*], Dae-Yeul Yu[4], and Hye Jin Choi[5]

[1]Department of Radiology, Samsung Medical Center, Sungkyunkwan University School of Medicine, Seoul;
[2]Department of Health Science and Technology, SAIHST, Sungkyunkwan University, Seoul;
[3]Department of Pharmacy, College of Pharmacy, Yonsei Institute of Pharmaceutical Science, Yonsei University, Incheon;
[4]Genome Editing Research Center, Korea Research Institute of Bioscience and Biotechnology (KRIBB), Daejeon;
[5]Division of Oncology, Department of Internal Medicine, Severance Hospital, Yonsei University College of Medicine, Seoul, Korea.

Purpose: Expression of organic anion transporting polypeptides (OATPs) 1B1/1B3 in hepatocellular carcinoma (HCC) induces a paradoxical enhancement of gadoxetic acid on liver magnetic resonance imaging (MRI). We examined the expression profile of OATPs with regard to tumor differentiation in a genetically modified H-Ras 12V mouse model of spontaneous HCC that undergoes multistep hepatocarcinogenesis with minimal inter-individual variation.

Materials and Methods: Tumor nodules were harvested from transgenic H-Ras 12V mice. Hematoxylin and eosin-stained slides were examined for tumor differentiation and high-grade pathological components (tumor necrosis, thickened trabeculae, or vascular invasion). Immunohistochemistry of OATP 1B1/1B3 was performed, and OATP expression was assessed.

Results: We examined well-differentiated HCCs (n=59) in which high-grade pathological components were absent (n=49) or present (n=10). Among the well-differentiated HCCs without high-grade pathological components (n=49), OATP expression was negative, weak positive, and moderate positive in 23, 17, and nine cases, respectively. Among the well-differentiated HCCs with high-grade pathological components (n=10), OATP expression was negative, weak positive, and moderate positive in one, two, and seven cases, respectively. The ratio of positive OATP 1B1/1B3 expressing tumors was higher in HCCs with high-grade pathological components than in those without high-grade pathological components (p=0.004).

Conclusion: Our findings support those of previous clinical studies that have reported the frequent appearance of gadoxetic acid-enhanced MRI in moderately differentiated HCC.

Key Words: Carcinoma, hepatocellular; gadolinium ethoxybenzyl DTPA; magnetic resonance imaging

INTRODUCTION

Gadoxetic acid (Primovist®, Bayer Schering Pharma AG, Berlin, Germany) is a magnetic resonance imaging (MRI) contrast agent specialized for liver imaging. Gadoxetic acid acts as both an extracellular contrast and hepatocyte selective contrast agent, and approximately half of the injected dose is internalized by hepatocytes and is subsequently excreted into the bile.[1,2] This unique property is attributed to the fact that gadoxetic acid is transported from the circulation into hepatocytes by organic anion transporting polypeptide (OATP) 1B1 and 1B3, which are carrier proteins exclusively expressed in functional hepatocytes.[3] Consequently, the normal liver parenchyma shows selective enhancement at the hepatobiliary phase, which improves the detection of focal liver lesions lacking functional hepatocytes.[4]

Multistep hepatocarcinogenesis involves the accumulation

Received: January 14, 2021 **Revised:** March 29, 2021
Accepted: April 6, 2021
Corresponding author: Hye Jin Choi, PhD, Department of Internal Medicine, Yonsei University College of Medicine, 50-1 Yonsei-ro, Seodaemun-gu, Seoul 03722, Korea.
Tel: 82-2-2228-8130, Fax: 82-2-393-3652, E-mail: choihj@yuhs.ac

*Honsoul Kim and Junjeong Choi contributed equally to this work.
•The authors have no potential conflicts of interest to disclose.

© Copyright: Yonsei University College of Medicine 2021
This is an Open Access article distributed under the terms of the Creative Commons Attribution Non-Commercial License (https://creativecommons.org/licenses/by-nc/4.0) which permits unrestricted non-commercial use, distribution, and reproduction in any medium, provided the original work is properly cited.

of epigenetic and genetic alterations and the occurrence of successive selection and expansion of less differentiated parent nodules.[5] The role of OATP1B1 and OATP1B3 signaling pathways in multistep hepatocarcinogenesis remains poorly understood, but their expression has been reported to decrease during the development of hepatocellular carcinoma (HCC).[6] The expression of these molecules is maintained in regenerating nodules and low-grade dysplastic nodules, but is low or absent in high-grade dysplastic nodules, early, and progressed HCCs.[7-9] The decrease in OATP expression can proceed portal venous flow reduction[10] and/or increase in arterial flow,[8] suggesting that the hepatobiliary phase enhancement may facilitate imaging-based diagnosis of HCC at earlier stages.[5]

However, multiple studies have reported the presence of an HCC subgroup in approximately 5–12% of the cases, which demonstrates paradoxical hyperintensity of gadoxetic acid in the hepatobiliary phase MRI images.[7,11-13] This subgroup has distinct features such as being biologically indolent, lower tumor grade, less frequent vascular invasion, and longer recurrence-free survival after resection.[12,14-16] However, whether paradoxical enhancement mainly occurs in well-differentiated HCC or moderately differentiated HCC remains unclear.[8,17-20] We speculate that the discrepancies among different studies may be the result of substantial inter-individual variation in the study populations, underlying liver diseases, predisposing factors, genetic background, and lifestyle that lead to heterogeneous HCC presentation.

In the current study, we used a genetically modified H-ras 12V mouse model of spontaneous HCC[21,22] to examine the expression profile of OATPs during tumor differentiation. Similar to HCC patients, these mice showed multistep hepatocarcinogenesis but with minimal inter-individual variation. A uniform oncogenic stimulus drives hepatocarcinogenesis in these mice, and the differences in genetic background and environment are negligible.

MATERIALS AND METHODS

This study was approved by the Institutional Animal Care and Use Committee of Yonsei University Severance Hospital (2017-0330), and the animal experiments were conducted in accordance with the National Institute of Health Guide for the Care and Use of Laboratory Animals.

Transgenic mice and treatment

H-Ras 12V transgenic mice were kindly provided by Professor Dae-Yeul Yu of Korea Research Institute of Bioscience and Biotechnology. Transgenic lines were established by mating these mice with C57BL/6 mice. Genotyping was performed using polymerase chain reaction (PCR) with forward primer 5'-CTAGGGCTGCAGGAATTC-3' and reverse primer 5'-GTAGTTTAACACATTATACACT-3'. PCR in transgenic mice yielded a 711 bp product.[23] All mice were fed a standard normal diet ad libitum with free access to water. Only male mice were used for experiments, and the mice were housed in a specific pathogen-free facility for up to 13 months to allow sufficient incubation time required for spontaneous hepatocarcinogenesis (Fig. 1).

MRI acquisition

Initially, nine mice were subjected to gadoxetic acid-enhanced MRI. The mice were scanned with a horizontal-bore 9.4T micro-MRI scanner (Biospec 94/20 USR, Bruker Biospin Inc., Billerica, MA, USA) while under general anesthesia. The mice were placed in an induction chamber, and anesthesia was induced with a mixture of 3% isoflurane and 97% oxygen. Then, anesthesia was maintained during imaging by supplying a mixture of 2% isoflurane and 99.2–98% oxygen at a flow rate of 1.5/min administered with an animal nose/mouth mask. All animals were positioned prone in a dedicated animal cradle heated via a thermostat-driven water bath. A pressure transducer consisting of a small air cushion was attached to the abdominal wall to monitor the respiratory rate during the MR procedures. For the contrast-enhanced study, 1.2 μL/g (body weight) gadoxetic acid (Primovist®) was injected through the tail vein. The dosage of gadoxetic acid was determined by multiplying the translation factor by the body surface area to the recommended human dosage.[24] Hepatobiliary phase images were obtained 15 min after contrast agent injection. To perform radiological-pathological correlation, the tumor samples were sampled and correlated with the corresponding nodules from the MRI images. However, upon dissection, many small tumors were crowded within the mouse liver tumors. Unlike the human liver, in which each lobe is fixed, the lobes of the mouse liver were separated while being connected only at the hilum (Fig. 1A). Consequently, the position of each lobe was different between the MR images and the dissected liver. This complicated the histological imaging correlation, especially if the nodules were small or crowded.

Histological examination and immunohistochemistry

Male mice (8–13 months old) were sacrificed under anesthesia to obtain tumor samples. For immunofluorescence, tumor samples were initially fixed in 4% paraformaldehyde overnight, incubated in 20% sucrose solution at 4°C overnight 10 μm thickness were cut, and anti-CD31 antibody (MAB1398Z, Millipore, Billerica, MA, USA) and Cy3-conjugated anti-smooth muscle actin (Sigma-Aldrich, St. Louis, MO, USA) were used for immunofluorescence. An LSM 510 confocal microscope equipped with argon and helium-neon lasers (Carl Zeiss, Oberkochen, Germany) was used to obtain images.

Tumor nodules in the liver were dissected and fixed in 10% buffered formalin overnight. Samples were then embedded in paraffin and sectioned at 5-mm intervals. The tumor nodule was matched during sampling with gadoxetic acid-enhanced MRI for the radiological-pathological correlation. Tumor nod-

ules that were difficult to correlate with the MRI images were marked.

Hematoxylin and eosin (H&E) staining and immunohistochemistry were performed using anti-OATP2 (synonymous with OATP1B1) and anti-OATP8 (synonymous with OATP1B3) antibodies (GTX15442, Genetex, Irvine, CA, USA). The slides

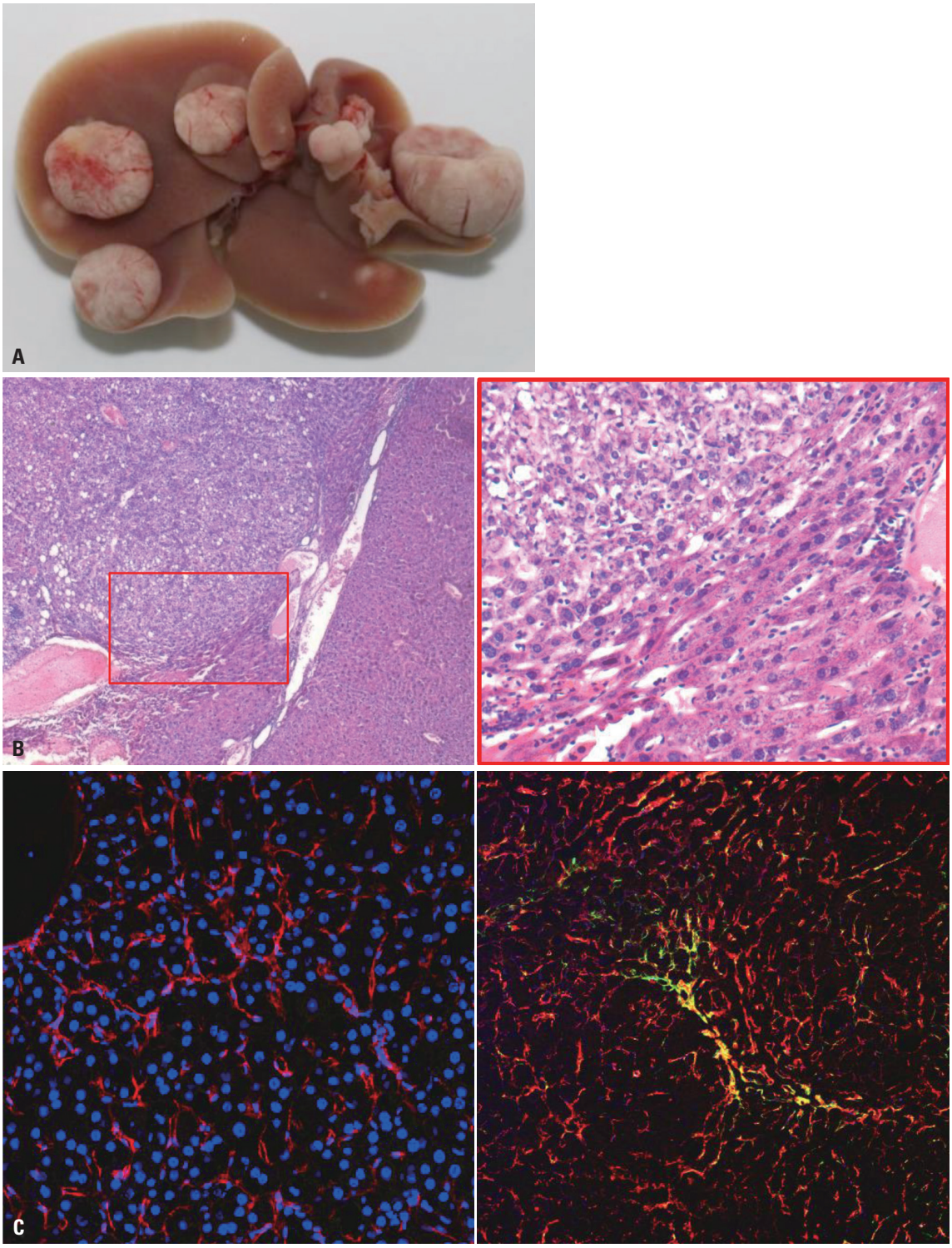

Fig. 1. Characterization of HCC spontaneously developed in an 8.5-month-old H-Ras 12V transgenic mouse. (A) Gross examination of the dissected liver revealed multiple tumor nodules. (B) Hematoxylin and eosin staining of the tumor periphery (magnification: left, ×40; right, ×200) revealed tumor cells with wide thickened trabeculae and mild cytologic atypia, similar to well-differentiated HCC. (C) Confocal images of immunofluorescence staining [left: CD 31 (red), DAPI (blue); right: smooth muscle actin (red), laminin (green)]. HCC, hepatocellular carcinoma.

https://doi.org/10.3349/ymj.2021.62.7.622

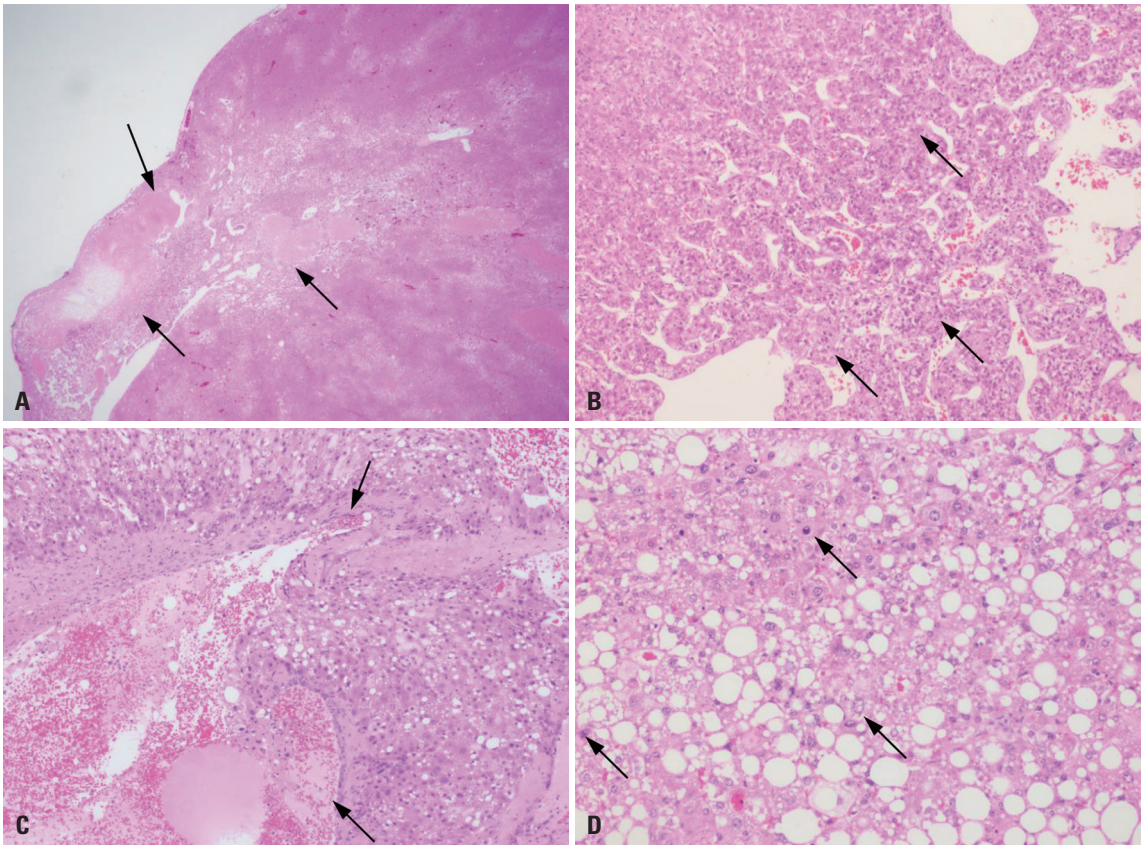

Fig. 2. Hematoxylin and eosin staining typical images of high-grade pathological components showing (A) widespread necrosis (arrows, magnification: ×12.5), (B) thickened trabeculae (arrows, magnification: ×40), (C) vascular invasion (arrows, magnification: ×40), and (D) presence of high-grade nuclear atypia (arrows, magnification: ×100).

were reviewed by a pathologist (J.C.) with 5 years of experience in experimental animal histopathology and human pathology.

Only nodules diagnosed as HCC based on the morphological features of the H&E-stained slides were analyzed. Tumor differentiation was assessed, and in the case of well-differentiated tumors, the presence or absence of high-grade pathological components such as tumor foci containing necrosis, thickened trabeculae, and vascular invasion in more than 10% of the tumor surface was marked (Fig. 2). Immunohistochemistry of OATP-stained slides was performed to grade the intensities of OATP expression. The intensity of OATP expression was categorized into three grades (grade 0: negative; grade 1: weak positive; and grade 2: moderate to strong positive). The extent of OATP expression within the tumor was categorized into three grades (grade 1: OATP expression was detected in less than 33% of the tumor; grade 2, between 33% and 67% of the tumor; grade 3, more than 67% of the tumor).

Statistical analysis

Statistical analysis was performed using SPSS v.25 (IBM Corp., Armonk, NY, USA). Fisher's exact test was performed to compare the rate of tumor differentiation and intensity of OATP 1B1/1B3 expression. Statistical significance was set at $p<0.05$.

RESULTS

Dissected livers from transgenic male mice with HCC at 8.5 months of age revealed the development of multiple nodules (Fig. 1A). The larger nodules revealed prominent vessels on their surface. Hematoxylin and eosin staining revealed multiple, well-vascularized nodules composed of well-differentiated tumor cells with wide thickened trabeculae and mild cytologic atypia (Fig. 1B). Confocal microscopy after immunofluorescence staining demonstrated increased expression of CD31, smooth muscle actin, and laminin in the tumor capillaries (Fig. 1C), but not in the sinusoidal capillaries. Based on these findings, we determined that the histological features of HCCs generated in this mouse model were similar to those of human HCC.

Next, we performed gadoxetic acid-enhanced MRI, which revealed 44 liver nodules in nine mice. Many of these nodules were small and close to each other, which made the radiological-pathological correlation difficult. Moreover, unlike the human liver, which has immovable lobes, the mouse liver consisted of separate lobes that were connected to each other only at the hilum (Fig. 1A); therefore, the position of each lobe was not consistent. As a result, we were not able to confidently match some of the nodules on the specimen during dissection with the baseline MRI. Therefore, that radiology-pathology

correlation was not performed.

In total, we harvested 59 HCCs from 13 male transgenic mice, and all of them were well-differentiated. Moderately and poorly differentiated HCCs were not detected. The tumors were further graded into well-differentiated HCCs without high-grade pathological components (n=49) and well-differentiated HCCs with high-grade pathological components (n=10) (Fig. 2). Among the well-differentiated HCCs without high-grade pathological components (n=49), OATP expression was negative, weak positive, and moderate positive in 46.9% (n=23/49), 34.7% (n=

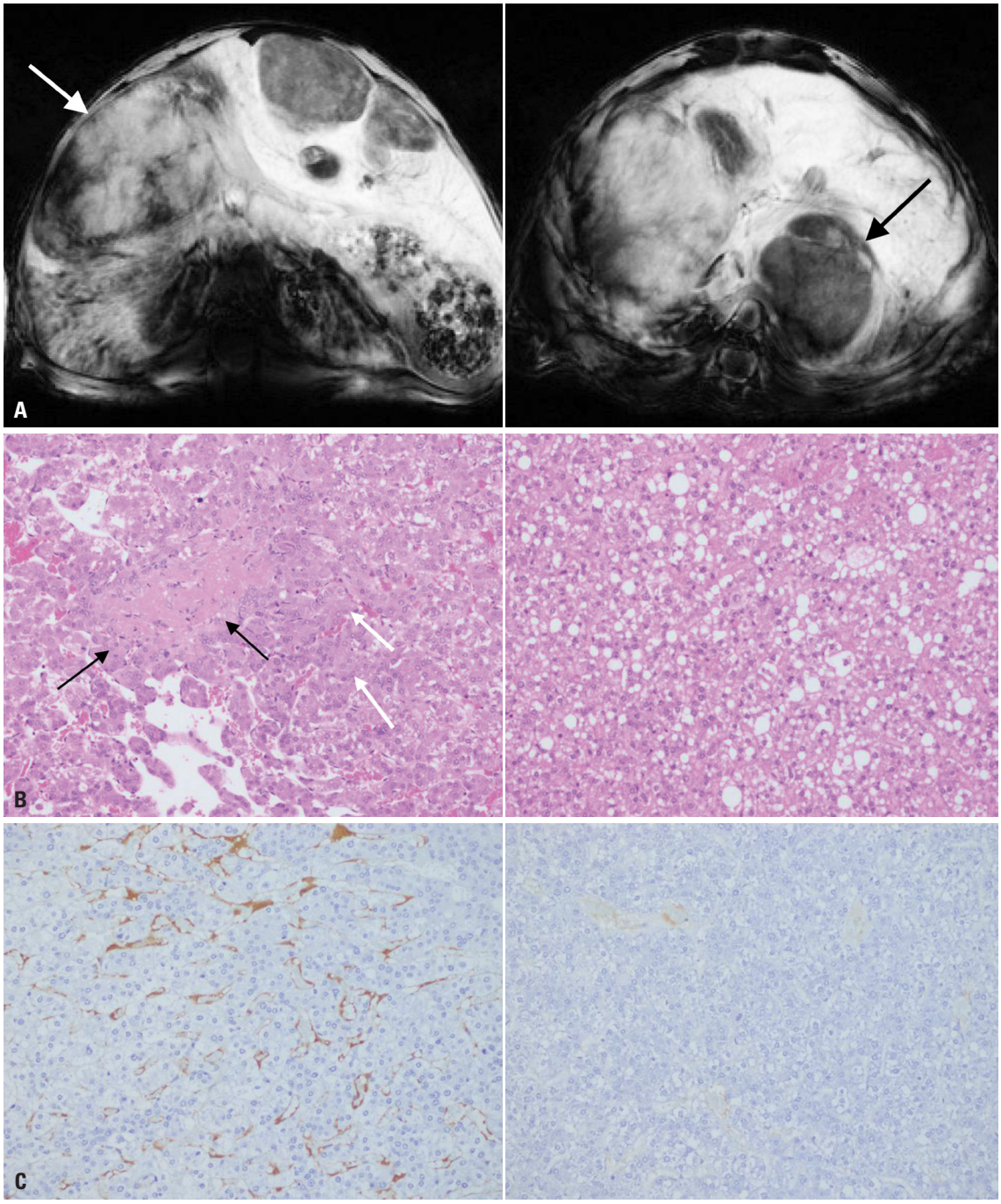

Fig. 3. HCC in 10-month-old male H-Ras 12V transgenic mice. (A) Representative fat-suppressed T1 weighted image, obtained 15 min after gadoxetic acid injection, demonstrates nodules with (left) mild enhancement (white arrow) and (right) without enhancement (black arrow). (B) Hematoxylin and eosin-stained image and (C) immunohistochemistry of OATP 1B1/1B3 (left column). The nodule with mild enhancement on MRI was a well-differentiated HCC with high-grade pathological components, such as necrosis (black arrows) and thick trabeculae (white arrows), and showed moderate positive OATP 1B1/1B3 expression (right column). The nodule without enhancement on MRI was a well-differentiated HCC without high-grade pathological components, and the OATP 1B1/1B3 expression was negative. HCC, hepatocellular carcinoma; OATP, organic anion transporting polypeptides; MRI, magnetic resonance imaging.

https://doi.org/10.3349/ymj.2021.62.7.622

Table 1. Profile of Tumor Differentiation and the Intensity and Extent of OATP 1B1/1B3 Expression

Tumor differentiation	Well-differentiated HCC without high grade pathological component			Well-differentiated HCC with high grade pathological components			*p* value
OATP intensity	Negative	Weak positive	Moderate positive	Negative	Weak positive	Moderate positive	
	23	17	9	1	2	7	0.004
OATP extent*	-	G1/G2/G3	G1/G2/G3	-	G1/G2/G3	G1/G2/G3	-
	-	10/5/2	1/1/7	-	1/0/1	0/2/5	-

OATP, organic anion transporting polypeptides; HCC, hepatocellular carcinoma.
*G1: OATP expression was detected in less than 33% of the tumor, G2: between 33% and 67% of the tumor, G3: more than 67% of the tumor.

17/49), and 18.4% (n=9/49) of the tumors, respectively (Fig. 3). In the 10 well-differentiated HCCs with high-grade pathological components, OATP expression was negative, weak positive, moderate positive in 10.0% (n=1/10), 20.0% (n=2/10), and 70.0% (n=7/10) of the tumors, respectively (Fig. 3). The well-differentiated HCCs with high-grade pathological components had a higher rate of positive OATP 1B1/1B3 expression compared to that of HCCs without high-grade pathological components (p= 0.004) (Table 1).

Among the 17 well-differentiated HCCs that showed weak positive OATP 1B1/1B3 expression, 10 tumors showed positive OATP expression in less than 33% of the tumor (grade 1), five tumors showed positive OATP expression in 33% to 67% (grade 2), and two tumors showed positive OATP expression in more than 67% of the tumor (grade 3). In the nine HCCs that showed moderate positive OATP expression, one, one, and seven tumors were grade 1, grade 2, and grade 3, respectively (Table 1).

In the well-differentiated HCCs with high-grade pathological components, the extent of OATP expression in the two OATP 1B1/1B3 weak positive tumors was grade 1 (n=1) and grade 3 (n=1) each. The extent of OATP 1B1/1B3 expression in the moderate positive HCCs was grade 2 and grade 3 in two and five tumors, respectively (Table 1).

DISCUSSION

During multistep hepatocarcinogenesis, more aggressive tumor clones with molecular alterations emerge within a less aggressive tumor or premalignant nodule.[25] As the increased numbers of aggressive tumor clones have a survival advantage, they will eventually replace the less aggressive precursor lesion, which can be detected during histological evaluation.[5,26] Mutations then successively accumulate, producing molecular derangements that may correlate with tumor differentiation. In this process, if molecular alterations influence the OATP 1B1/1B3 signaling pathway, the enhancement of gadoxetic acid on HCC hepatobiliary phase MRI images may theoretically reveal a definable pattern linked to tumor differentiation. For instance, OATP1B3 has been reported to interact with hepatocyte nuclear factor 4α, forkhead box M1, and β-catenin signaling pathways.[6,27-31] Kitao, et al.[6] reported that hyperintense (OATP1B3-high) HCC and hypointense (OATP1B3-low) HCC can represent genetically different subtypes.

It is well-known that the hepatobiliary phase enhancement of gadoxetic acid-enhanced MRI correlates with the degree of OATP1B3 expression in HCC, and therefore is considered as an indirect molecular imaging marker.[5,6,13] Previous studies have reported that hepatobiliary phase hyperintense HCC demonstrate more frequent pseudoglandular proliferation pattern and bile plug formation, and lower rate of portal vein invasion rate.[6,12] Hepatobiliary phase hyperintense HCCs were also associated with lower levels of tumor markers such as alpha fetoprotein and protein induced by vitamin K absence or antagonist.[6,12,32,33] Moreover, hepatobiliary phase hyperintense HCCs showed lower recurrence rate and longer survival after surgical resection.[6,12,32-34]

Most HCCs demonstrate decreased signal intensity in the hepatobiliary phase of gadoxetic acid-enhanced MRI, but paradoxical enhancement occurs in a subgroup of HCC.[7,11-13] However, the relationship between tumor differentiation and hepatobiliary phase enhancement has been controversial. Some researchers have reported that such paradoxical enhancement is limited to well-differentiated HCCs,[18,19,35] whereas others have indicated that it also occurs in moderately differentiated HCCs.[17] One study claimed that no correlation existed between paradoxical enhancement and HCC differentiation.[20] Meanwhile, other studies have indicated that paradoxical enhancement is predominately associated with moderately differentiated HCCs.[8,13,36]

The hepatobiliary enhancement that was observed only in well-differentiated HCCs[18,19,35] seem plausible as the hepatobiliary enhancement may be localized in the initial benign nodules of well-differentiated HCC where physiological levels of OATP 1B1/1B3 is maintained. It can be hypothesized that OATP 1B1/1B3 activity diminishes as hepatocarcinogenesis progresses to worsen tumor differentiation. In contrast, studies describing paradoxical enhancement as an event predominantly appearing in moderately differentiated HCCs[8,13,36] are somewhat more challenging to explain, as this suggests that OATP 1B1/1B3 expression has to fluctuate by being temporally suppressed (well-differentiated stage), reactivated (moderately differentiated stage), and then again suppressed (poorly differentiated stage). Alternatively, some researchers have simply explained this as enhanced HCCs developing from hypointense borderline lesions due to genetic or epigenetic alterations.[6,13]

We speculated that such contradicting observations could be, at least partly, influenced by observational errors caused by substantial inter-individual variation among study populations. Different predisposing factors, such as oncogenic stimuli, genetic background, and environmental factors, may also contribute to the observational differences. The combined effect of these variations may have had an impact on the multistep hepatocarcinogenesis and OATP 1B1/1B3 signaling pathways, complicating the HCC enhancement profile of gadoxetic acid-enhanced MRI and its relationship with tumor differentiation.

Based on this perspective, we examined the relationship between tumor differentiation and OATP 1B1/1B3 expression profiles in a standardized system in which HCC develops under uniform stimulus with minimal inter-individual variations. We used the H-Ras 12V transgenic mice as we speculated that this model would develop HCC driven by a uniform oncogenic stimulus (H-Ras oncogene) at a relatively consistent amplitude. Moreover, as these mice are syngeneic, they have little difference in genetic background. The mice feed on the same diet and live in an identical environment, unlike human patients; therefore, the differences in environmental factors and lifestyle are negligible. Therefore, we hypothesized that this mouse model should have minimal inter-individual differences and could help clarify the relationship between tumor differentiation and OATP 1B1/1B3 expression.

Before immunohistochemistry, we first examined the histological features of HCCs generated in H-Ras 12V transgenic mice to validate the tumor model. Hematoxylin and eosin staining revealed morphological similarities with those of human HCCs, such as thickened trabeculae with cytologic atypia and capillarization. Occasional necrotic foci and thick cords of tumor cells were also observed. Immunofluorescence staining revealed prominent expression of CD31, laminin, and smooth muscle actin in the tumor capillaries, indicating that sinusoidal capillarization and arterialization had occurred.[37] The HCCs generated in this mouse model have been described to induce the formation of tumor-feeding vessels from the hepatic artery that gradually replace the physiologic portal venous perfusion, similar to human HCC patients.[23] One study on gadoxetic acid-enhanced MRI using this mouse model reported that the HCCs mostly revealed low signal intensity on T1 weighted images after enhancement in the delayed phase, but 16.1% of the lesions presented with nodule-in-nodule appearance.[21] Based on these results and studies, we concluded that the HCCs generated in the H-Ras 12V mice closely resemble the histologic, vascular, and MRI features of human HCC. Therefore, these mice can serve as a robust experimental platform for recapitulating human HCC.

Next, we harvested 59 HCCs, which were all confirmed as well-differentiated tumors. The majority of the tumors were well-differentiated HCCs without high-grade pathological components (n=49), but some HCCs (n=10) contained high-grade pathological components. As both OATP1B3 and OATP1B1 transports gadoxetic acid into hepatocytes and therefore enhances the hepatobiliary phase,[3,38] we performed immunohistochemistry with an antibody cross-reactive for both carrier proteins. Approximately half of the well-differentiated HCCs without high-grade pathological components were OATP 1B1/1B3 negative (46.9%; n=23/49), whereas only 10.0% (n=1/10) of well-differentiated HCCs with high-grade pathological components were OATP 1B1/1B3 negative. In contrast, the proportion of OATP 1B1/1B3 moderate-intensity HCCs was 18.4% (n=9/49) in well-differentiated HCCs without high-grade pathological components, but 70.0% (n=7/10) in well-differentiated HCCs with high-grade pathological components (Table 1 and Fig. 4). We believe that the higher ratio of OATP 1B1/1B3-positive HCC observed in well-differentiated HCCs with high-grade pathological components indicates that OATP 1B1/1B3-positive tumor cells must have increased as tumor differentiation worsened. Therefore, our observation supports the results of a previous clinical study that reported paradoxical enhancement of the hepatobiliary phase of gadoxetic acid-enhanced MRI to be a phenomenon that is predominantly associated with moderately differentiated HCCs.[8]

Our study had a few limitations. First, we used a genetically modified mouse to establish HCC. However, the HCC pathogenesis in this mouse model was different compared to that in humans, in which various underlying diseases, such as chronic viral hepatitis, induce HCC. Nevertheless, we specifically selected a standardized tumor model driven by a uniform oncogenic stimulus to minimize inter-individual variation. Second, as mentioned above, we were not able to perform a radiology-

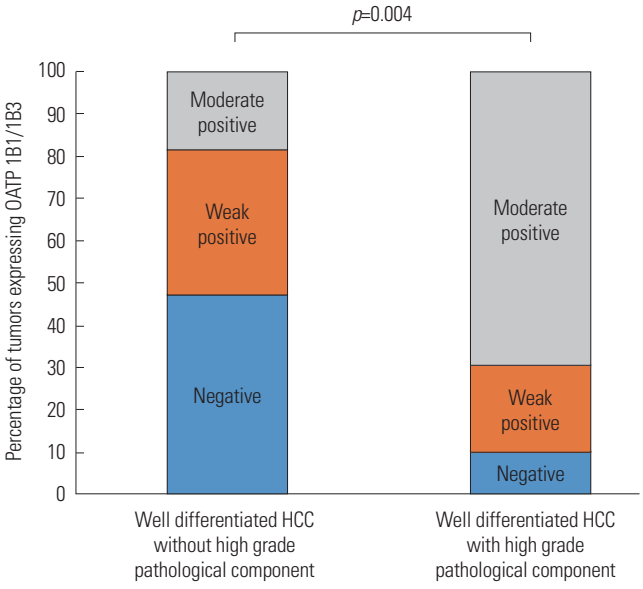

Fig. 4. Schematic graph depicting the relation between the presence or absence of high-grade pathological tumor component and OATP 1B3/1B1 expression. OATP, organic anion transporting polypeptides; HCC, hepatocellular carcinoma.

https://doi.org/10.3349/ymj.2021.62.7.622

pathology correlation, since we could not confidently differentiate the tumors crowded within the small liver and match them on the MRI. However, considering the importance of OATP 1B1/1B3 in liver imaging, we believe that examining the expression pattern of these molecules in a standardized mouse HCC model is still meaningful. Third, our model only produced well-differentiated HCCs, and therefore, poorly differentiated HCCs were not examined. We believe that the short life span of the mice did not allow sufficient incubation time for the tumors to undergo multistep hepatocarcinogenesis to generate poorly differentiated tumors. However, most of the controversy regarding the OATP expression pattern in HCC was focused on the well-differentiated and moderately differentiated stages, and not the poorly differentiated stage of tumors. Therefore, we considered the inability of our model to produce poorly differentiated HCC as a minor limitation. In our study, we divided the well-differentiated HCCs according to the presence or absence of high-grade pathological components for comparison of tumor differentiation.

In conclusion, well-differentiated HCCs generated in H-Ras 12V transgenic mice revealed an increased OATP 1B1/1B3 expression ratio in tumors with high-grade pathological components. Our results support clinical studies that reported paradoxical hepatobiliary phase enhancement of gadoxetic acid-enhanced MRI in moderately differentiated HCC.

ACKNOWLEDGEMENTS

This work was supported by a National Research Foundation of Korea (NRF) grant funded by the Korean government (No. NRF-2017R1D1A1B03035611).

AUTHOR CONTRIBUTIONS

Conceptualization: Honsoul Kim, Junjeong Choi, and Hye Jin Choi. Data curation: Honsoul Kim and Junjeong Choi. Formal analysis: Honsoul Kim and Junjeong Choi. Funding acquisition: Hye Jin Choi. Investigation: Honsoul Kim. Methodology: Honsoul Kim, Junjeong Choi, and Dae-Yeul Yu. Project administration: Hye Jin Choi. Resources: Dae-Yeul Yu and Hye Jin Choi. Software: Honsoul Kim. Supervision: Junjeong Choi and Hye Jin Choi. Validation: Junjeong Choi and Hye Jin Choi. Visualization: Honsoul Kim and Junjeong Choi. Writing—original draft: Honsoul Kim. Writing—review & editing: Junjeong Choi and Hye Jin Choi. Approval of final manuscript: all authors.

ORCID iDs

Honsoul Kim https://orcid.org/0000-0002-2367-234X
Junjeong Choi https://orcid.org/0000-0003-1339-593X
Dae-Yeul Yu https://orcid.org/0000-0003-0399-4234
Hye Jin Choi https://orcid.org/0000-0001-5917-1400

REFERENCES

1. Van Beers BE, Pastor CM, Hussain HK. Primovist, Eovist: what to expect? J Hepatol 2012;57:421-9.
2. Bartolozzi C, Crocetti L, Lencioni R, Cioni D, Della Pina C, Campani D. Biliary and reticuloendothelial impairment in hepatocarcinogenesis: the diagnostic role of tissue-specific MR contrast media. Eur Radiol 2007;17:2519-30.
3. Leonhardt M, Keiser M, Oswald S, Kühn J, Jia J, Grube M, et al. Hepatic uptake of the magnetic resonance imaging contrast agent Gd-EOB-DTPA: role of human organic anion transporters. Drug Metab Dispos 2010;38:1024-8.
4. Huppertz A, Balzer T, Blakeborough A, Breuer J, Giovagnoni A, Heinz-Peer G, et al. Improved detection of focal liver lesions at MR imaging: multicenter comparison of gadoxetic acid-enhanced MR images with intraoperative findings. Radiology 2004;230:266-75.
5. Choi JY, Lee JM, Sirlin CB. CT and MR imaging diagnosis and staging of hepatocellular carcinoma: part I. Development, growth, and spread: key pathologic and imaging aspects. Radiology 2014;272:635-54.
6. Kitao A, Matsui O, Yoneda N, Kozaka K, Kobayashi S, Koda W, et al. Gadoxetic acid-enhanced MR imaging for hepatocellular carcinoma: molecular and genetic background. Eur Radiol 2020;30:3438-47.
7. Cho ES, Choi JY. MRI features of hepatocellular carcinoma related to biologic behavior. Korean J Radiol 2015;16:449-64.
8. Kitao A, Matsui O, Yoneda N, Kozaka K, Shinmura R, Koda W, et al. The uptake transporter OATP8 expression decreases during multistep hepatocarcinogenesis: correlation with gadoxetic acid enhanced MR imaging. Eur Radiol 2011;21:2056-66.
9. Vavricka SR, Jung D, Fried M, Grützner U, Meier PJ, Kullak-Ublick GA. The human organic anion transporting polypeptide 8 (SLCO1B3) gene is transcriptionally repressed by hepatocyte nuclear factor 3β in hepatocellular carcinoma. J Hepatol 2004;40:212-8.
10. Kogita S, Imai Y, Okada M, Kim T, Onishi H, Takamura M, et al. Gd-EOB-DTPA-enhanced magnetic resonance images of hepatocellular carcinoma: correlation with histological grading and portal blood flow. Eur Radiol 2010;20:2405-13.
11. Suh YJ, Kim MJ, Choi JY, Park YN, Park MS, Kim KW. Differentiation of hepatic hyperintense lesions seen on gadoxetic acid-enhanced hepatobiliary phase MRI. AJR Am J Roentgenol 2011;197:W44-52.
12. Kitao A, Matsui O, Yoneda N, Kozaka K, Kobayashi S, Koda W, et al. Hypervascular hepatocellular carcinoma: correlation between biologic features and signal intensity on gadoxetic acid-enhanced MR images. Radiology 2012;265:780-9.
13. Narita M, Hatano E, Arizono S, Miyagawa-Hayashino A, Isoda H, Kitamura K, et al. Expression of OATP1B3 determines uptake of Gd-EOB-DTPA in hepatocellular carcinoma. J Gastroenterol 2009;44:793-8.
14. Vasuri F, Golfieri R, Fiorentino M, Capizzi E, Renzulli M, Pinna AD, et al. OATP 1B1/1B3 expression in hepatocellular carcinomas treated with orthotopic liver transplantation. Virchows Arch 2011;459:141-6.
15. Choi JY, Lee JM, Sirlin CB. CT and MR imaging diagnosis and staging of hepatocellular carcinoma: Part II. Extracellular agents, hepatobiliary agents, and ancillary imaging features. Radiology 2014;273:30-50.
16. Lee SA, Lee CH, Jung WY, Lee J, Choi JW, Kim KA, et al. Paradoxical high signal intensity of hepatocellular carcinoma in the hepatobiliary phase of Gd-EOB-DTPA enhanced MRI: initial experience. Magn Reson Imaging 2011;29:83-90.
17. Kim SH, Kim SH, Lee J, Kim MJ, Jeon YH, Park Y, et al. Gadoxetic acid-enhanced MRI versus triple-phase MDCT for the preoperative detection of hepatocellular carcinoma. AJR Am J Roentgenol 2009;192:1675-81.
18. Huppertz A, Haraida S, Kraus A, Zech CJ, Scheidler J, Breuer J, et

al. Enhancement of focal liver lesions at gadoxetic acid-enhanced MR imaging: correlation with histopathologic findings and spiral CT--initial observations. Radiology 2005;234:468-78.
19. Ni Y, Marchal G, Yu J, Mühler A, Lukito G, Baert AL. Prolonged positive contrast enhancement with Gd-EOB-DTPA in experimental liver tumors: potential value in tissue characterization. J Magn Reson Imaging 1994;4:355-63.
20. Asayama Y, Tajima T, Nishie A, Ishigami K, Kakihara D, Nakayama T, et al. Uptake of Gd-EOB-DTPA by hepatocellular carcinoma: radiologic-pathologic correlation with special reference to bile production. Eur J Radiol 2011;80:e243-8.
21. Bang DH, Park SH, Jun HY, Moon HB, Kim SU, Yu DY, et al. Gd-EOB-DTPA enhanced micro-MR imaging of hepatic tumors in H-ras 12V transgenic mice. Acad Radiol 2011;18:13-9.
22. Wang AG, Moon HB, Lee MR, Hwang CY, Kwon KS, Yu SL, et al. Gender-dependent hepatic alterations in H-ras12V transgenic mice. J Hepatol 2005;43:836-44.
23. Kim SK, Kim H, Koh GY, Lim DS, Yu DY, Kim MD, et al. Mouse hepatic tumor vascular imaging by experimental selective angiography. PLoS One 2015;10:e0131687.
24. Reagan-Shaw S, Nihal M, Ahmad N. Dose translation from animal to human studies revisited. FASEB J 2008;22:659-61.
25. Farazi PA, DePinho RA. Hepatocellular carcinoma pathogenesis: from genes to environment. Nat Rev Cancer 2006;6:674-87.
26. Narsinh KH, Cui J, Papadatos D, Sirlin CB, Santillan CS. Hepatocarcinogenesis and LI-RADS. Abdom Radiol (NY) 2018;43:158-68.
27. Halilbasic E, Claudel T, Trauner M. Bile acid transporters and regulatory nuclear receptors in the liver and beyond. J Hepatol 2013;58:155-68.
28. Wang X, Kiyokawa H, Dennewitz MB, Costa RH. The Forkhead Box m1b transcription factor is essential for hepatocyte DNA replication and mitosis during mouse liver regeneration. Proc Natl Acad Sci U S A 2002;99:16881-6.
29. Bonzo JA, Ferry CH, Matsubara T, Kim JH, Gonzalez FJ. Suppression of hepatocyte proliferation by hepatocyte nuclear factor 4α in adult mice. J Biol Chem 2012;287:7345-56.
30. Ning BF, Ding J, Yin C, Zhong W, Wu K, Zeng X, et al. Hepatocyte nuclear factor 4α suppresses the development of hepatocellular carcinoma. Cancer Res 2010;70:7640-51.
31. Kitao A, Matsui O, Yoneda N, Kozaka K, Kobayashi S, Koda W, et al. Gadoxetic acid-enhanced magnetic resonance imaging reflects co-activation of β-catenin and hepatocyte nuclear factor 4α in hepatocellular carcinoma. Hepatol Res 2018;48:205-16.
32. Choi JW, Lee JM, Kim SJ, Yoon JH, Baek JH, Han JK, et al. Hepatocellular carcinoma: imaging patterns on gadoxetic acid-enhanced MR Images and their value as an imaging biomarker. Radiology 2013;267:776-86.
33. Miura T, Ban D, Tanaka S, Mogushi K, Kudo A, Matsumura S, et al. Distinct clinicopathological phenotype of hepatocellular carcinoma with ethoxybenzyl-magnetic resonance imaging hyperintensity: association with gene expression signature. Am J Surg 2015;210:561-9.
34. Yamashita T, Kitao A, Matsui O, Hayashi T, Nio K, Kondo M, et al. Gd-EOB-DTPA-enhanced magnetic resonance imaging and alpha-fetoprotein predict prognosis of early-stage hepatocellular carcinoma. Hepatology 2014;60:1674-85.
35. Tsuda N, Kato N, Murayama C, Narazaki M, Yokawa T. Potential for differential diagnosis with gadolinium-ethoxybenzyl-diethylenetriamine pentaacetic acid-enhanced magnetic resonance imaging in experimental hepatic tumors. Invest Radiol 2004;39:80-8.
36. Kitao A, Zen Y, Matsui O, Gabata T, Kobayashi S, Koda W, et al. Hepatocellular carcinoma: signal intensity at gadoxetic acid-enhanced MR imaging--correlation with molecular transporters and histopathologic features. Radiology 2010;256:817-26.
37. Yang ZF, Poon RT. Vascular changes in hepatocellular carcinoma. Anat Rec (Hoboken) 2008;291:721-34.
38. Nassif A, Jia J, Keiser M, Oswald S, Modess C, Nagel S, et al. Visualization of hepatic uptake transporter function in healthy subjects by using gadoxetic acid-enhanced MR imaging. Radiology 2012;264:741-50.

https://doi.org/10.3349/ymj.2021.62.7.622